Raman study of surface optical phonons in ZnO(Co) nanoparticles prepared by hydrothermal method

Branka Hadžić[1], Nebojša Romčević[1], Maja Romčević[1], Izabela Kuryliszyn-Kudelska[2], Witold D. Dobrowolski[2], Ursula Narkiewicz[3], Daniel Sibera[3]

[1]*Institute of Physics, University of Belgrade, Belgrade, Serbia*
[2]*Institute of Physics, Polish Academy of Science, Warsaw, Poland*
[3]*Institute of Chemical and Environment Engineering, Szczecin University of Technology, Szczecin, Poland*

Abstract
Raman scattering spectra of nanocrystalline samples of ZnO(Co) prepared by microwave-assisted hydrothermal synthesis were obtained and surface optical phonons (SOP) where observed in the range of 519–572 cm^{-1}. The mean crystalline size (33–300 nm) as well as the phase composition of obtained samples (ZnO and $ZnCo_2O_4$) were determined by X-ray diffraction measurements. These measurements allowed us to study the change of SOP modes position with crystalline size and how the change in concentration of doping component CoO affects the change of SOP modes intensity.

Keywords: nanostructured materials; optical properties; light absorption and reflection, surface optical phonon modes.

Available online at the Journal website: http://www.ache.org.rs/HI/

SCIENTIFIC PAPER

UDC 66.017/.018:54:543.424.2:53

Hem. Ind. **67** (4) 695–701 (2013)

doi: 10.2298/HEMIND121022119H

Diluted magnetic semiconductors (DMS) have attracted great interest recently due to their properties combining both spin and charge transport. With these characteristics, DMS are one of the most promising materials for spintronics [1,2]. Increasing attention has been devoted to nanostructures made of ZnO doped with transition metals such as Co, Ni, Cr, Fe and V after theoretical prediction of room temperature ferromagnetism in such systems [3–5]. Nanoparticles induce ferromagnetism in the host semiconductor material, if they contain inclusions of nanoscale oxides of transition metals [6] and/or a large concentration of magnetic ions [7].

Among other techniques, Raman spectroscopy is a convenient, non-destructive tool for gaining information about vibrational properties of ZnO, because of its ability to probe the local atomic arrangement around foreign elements, sample quality, information about phonon life times, isotopic effects and electron–-phonon coupling [8,9]. For this reason, it is used with for bulk crystals, nanocrystals and thin films, of both the pure host material and the crystal containing impurities. Besides the local atomic arrangement and dopant incorporation, in ZnO and ZnO-related compounds Raman scattering has also been used to study phonon processes, temperature dependence of Raman active modes, influence of annealing process, electron-phonon coupling, etc.[10–15].

Correspondence: N. Romčević, Institute of Physics, University of Belgrade, Pregrevica 118, 11080 Belgrade, Serbia.
E-mail: romcevi@ipb.ac.rs
Paper received: 22 October, 2012
Paper accepted: 21 November, 2012

In samples with large surface-to-volume ratios, the appearance of surface optical phonons (SOP) is expected in their Raman spectra, such as in the case of ZnO nanostructures. The existence of SOP modes has been predicted theoretically and/or detected experimentally for ZnO nanostructures [16]. When the dimensions become extremely small, the only mode that persists is a surface mode, which is why the state of surface atoms plays a key role in determining their properties. In ZnO nanostructures, one can expect loss of long-range order and symmetry breakdown in the ZnO shell, which causes the appearance of forbidden Raman modes. With this in mind we can say that those forbidden Raman modes are SOP modes [17].

The aim of this work is to study sample characteristics, position of the Co ion in the ZnO lattice, formation of existing phases, presence of SOP modes and the sample quality dependence on CoO concentration, by applying micro-Raman spectroscopy.

SAMPLES AND CHARACTERIZATION

The nanocrystalline samples of ZnO doped with CoO were obtained by hydrothermal synthesis. In this method a mixture of cobalt and zinc hydroxides was obtained by addition of an ammonia solution or 2 M solution of KOH to the 20% solution of a proper amount of $Zn(NO_3)\cdot 6H_2O$ and $Co(NO_3)\cdot 4H_2O$ in water. Next, the obtained hydroxides were put in the reactor with microwave emission. The microwave-assisted synthesis was conducted under a pressure of 3.8 MPa for 15 min. The synthesized product was filtered and dried.

This method obtained a series of nanosized ZnO samples with nominal concentration of CoO from 5% to

50%. The morphology of the samples was investigated using scanning electron microscopy (SEM). In SEM images of samples of lower CoO concentration, one can notice particles of similar size that belong to both registered phases, ZnO and $ZnCo_2O_4$. With increase in CoO concentration, the particle size becomes quite different, so we can easily distinguish two types of particles with diverse sizes: bigger (100 nm or more) belonging to the ZnO phase, and smaller, belonging to the $ZnCo_2O_4$ phase.

X-Ray diffraction (XRD) ($Co_{K\alpha}$ radiation, X'Pert Philips) was used to determine the phase composition of samples. The detailed phase composition investigations, in samples prepared by hydrothermal method, revealed the presence of crystalline phases of hexagonal ZnO and spinel structure $ZnCo_2O_4$ (ICSD: 23-1390). XRD data, obtained in this way, allowed us to determine a mean crystalline size, using Scherrer's formula [18], in these samples. Here the mean crystalline sizes d were between 64 and 300 nm for ZnO phases and from 33 to 77 nm for $ZnCo_2O_4$ phases. The obtained results of XRD measurements, phase composition and mean crystalline size are gathered in Table 1.

Table 1. XRD Analysis results for samples prepared by hydrothermal method. The identified crystalline phases and mean crystalline size, d, were determined using Scherrer's formula

Concentration of CoO mass%	*d* / nm	
	ZnO phase	$ZnCo_2O_4$ phase
5	65	48
10	64	33
20	65	37
30	100	55
40	100	77
50	300	40

The results of SEM and XRD analyses indicate that the crystalline size of ZnO increased with increasing CoO concentration, while the second phase $ZnCo_2O_4$ did not have a monotonous dependence. Further, it is obvious that the relative change of crystaline size of the $ZnCo_2O_4$ phase is smaller than the corresponding change of the ZnO phase.

Here we present the investigation of all samples obtained by hydrothermal method. No other crystal phases have been observed in the samples.

Surface optical phonons

The presence of surface optical phonons (SOP) is common for samples containing particles of nanoscale dimensions and containing imperfections, impurity, valence band mixing, etc. These characteristics result in loss of long-range order and symmetry breakdown with a rise of new, previously forbidden, vibration modes in Raman spectra whose phonons have $l \neq 0$ [10,11,19,20]. Another important characteristic of SOP modes is that they exist in polar crystals and that the wavelength of the incident laser beam needs to be larger than the particle size [17]. To understand how SOP modes behave, their characteristics and properties, a physical model is needed. This physical model has to describe the macroscopic properties of a medium based on the properties and relative fractions of its components. This kind of model is found in effective medium theory (EMT) [21]. In the literature, many different approximations of EMT can be found, each of them being more or less accurate in distinct conditions [17,21]. For polar semi-insulating semiconductors, among many approximations and mixing models for the effective dielectric permittivity [22], it seems that the Maxwell-Garnet approximation and mixing rule are most prominent [23,24]. As the Maxwell-Garnet approximation is only valid for small volume fractions of inclusions, it is not appropriate for our samples. Another famous and prominent approximation is the Bruggerman approximation and mixing rule [25–27], which is more adequate in the case of our samples. The Bruggeman model is more suitable for high concentrations of inclusions, because there are no restrictions for volume fraction in it. According to the Bruggeman mixing rule, the effective dielectric function is given by:

$$(1-f)\frac{\varepsilon_1-\varepsilon_{\text{eff}}}{\varepsilon_{\text{eff}}+g(\varepsilon_1-\varepsilon_{\text{eff}})}+f\frac{\varepsilon_2-\varepsilon_{\text{eff}}}{\varepsilon_{\text{eff}}+g(\varepsilon_2-\varepsilon_{\text{eff}})}=0 \qquad (1)$$

where g is a geometric factor who depends on the shape of the inclusions. In the case of three-dimensional spherical particles g = 1/3 and in the case of two-dimensional circles g = 1/2. The method of preparation and derivation of our samples results in clusterized nanoparticles, which occupy a considerably important volume. With all this in mind it is clear that our nanoparticles, when g = 1/3 is applied, satisfy the Bruggeman formula conditions.

In this case, it is necessary to take into account two phonons, typical for ZnO nanoparticles, which are in the region of SOP modes appearance, $\omega_{A_{1LO}} = 577\ \text{cm}^{-1}$, $\omega_{A_{1TO}} = 379\ \text{cm}^{-1}$, $\omega_{E_{1TO}} = 410\ \text{cm}^{-1}$, $\omega_{E_{1LO}} = 592\ \text{cm}^{-1}$, with dielectric permittivity $\varepsilon_\infty = 3.7$ [28–30]. Our samples are characterized by low concentration of free carriers and their low mobilities, which permits us to neglect influence of plasmon-phonon interaction. Another consequence of the preparation method in our samples is the random distribution of nanoparticles in space and thus to the incident light. In the obtained Raman spectra, as will be seen later, there is no E1 symmetry phonon, while the existence of A1 symmetry phonon has been registered. This observation can point out the assumption that the E1 symmetry phonon participates in SOP creation. The Raman intensities due to

excitation of extraordinary phonons, for our sample, are given by:

$$I \sim \mathrm{Im}(-\varepsilon_{\mathrm{eff}}) \quad (2)$$

In the area of Bruggerman formula applicability, this manner of calculation predicts appearance of one asymmetric peak, with wavenumbers below $\omega_{E1}(LO)$. This is in good agreement with the experimental spectra of ZnO doped with CoO nanopowders prepared by the hydrothermal method. Therefore, as a result of variation in the main volume fraction and damping rate, there great difference in the intensities and line shapes of simulated SOP modes.

RESULTS AND DISCUSSION

The micro-Raman spectra were taken in the back-scattering configuration and analyzed using a Jobin Yvon T64000 spectrometer, equipped with a nitrogen cooled charge-coupled-device detector. As an excitation source, the 514.5 nm line of an Ar-iron laser was used. The measurements were performed at 20 mW laser power.

The obtained Raman spectra have been analyzed using Lorentzian type lines for all phonons [31] while for calculations of SOP lines we have used Eqs. (1) and (2) with ε_1 = 1 (air). The obtained Raman spectra for all samples of nanocrystaline ZnO doped with CoO are shown in Figure 1. In these samples, as mentioned earlier, only nanoparticles of ZnO and $ZnCo_2O_4$ were registered with XRD. We will start our analysis of the obtained Raman spectra with brief report about structural and vibration properties of all potentially present phases in the samples, typical for bulk materials, which is absolutely necessary for understanding the vibration properties of nanoparticles. As a consequence of the nano-nature (structure) of our samples, we expect that bulk modes will be shifted and broadening.

ZnO, the basic material in our samples, is one of the simplest uniaxial, hexagonal crystals; a semiconductor with wurtzite structure belonging to the C_{6v}^4 space group. It has four atoms per primitive cell, all occupying

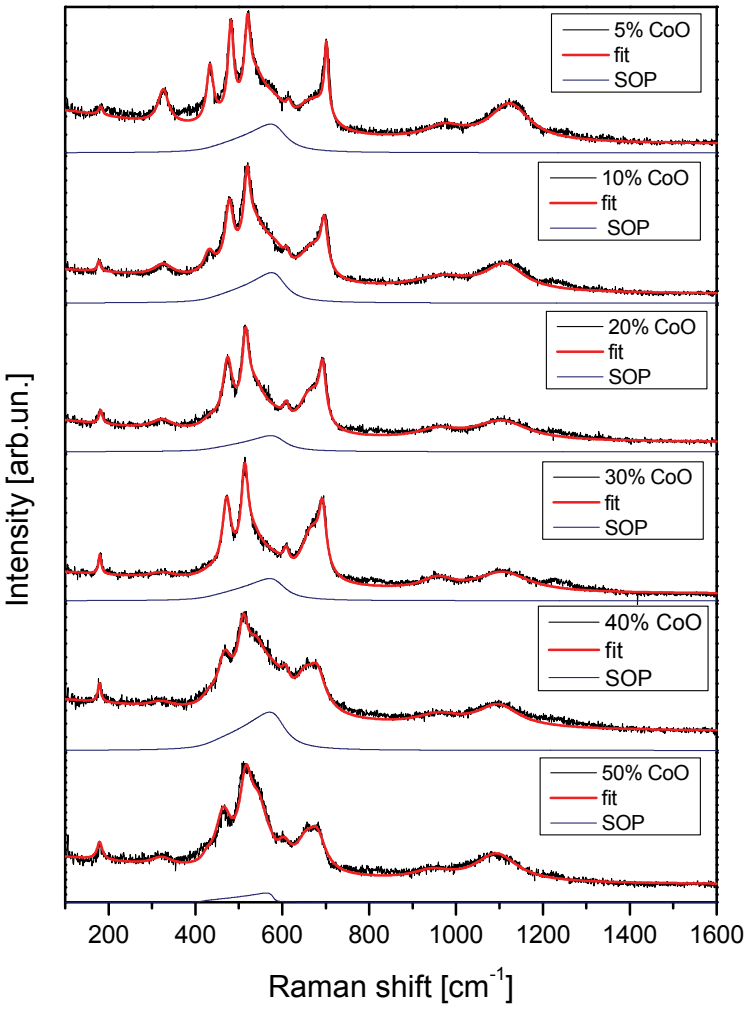

Figure 1. Fitted Raman spectra of nanocrystalline ZnO doped with CoO prepared by hydrothermal method. SOP modes are marked with solid lines.

C_{3v} sites. For a perfect ZnO crystal, only the optical phonons at the Γ point of the Brillouin zone are involved in first-order Raman scattering. Group theory predicts the existence of the following optical modes:

$$\Gamma_{opt} = A_1 + 2B_1 + E_1 + 2E_2$$

where A_1, E_1 and $2E_2$ modes are first-order Raman active, while the B_1 modes are Raman inactive modes [32,33]. Furthermore, the A_1 and E_1 modes are polar and can be further split into transverse optical (TO) and longitudinal optical (LO) phonons. The existence of macroscopic electric fields results in that the TO and LO phonons have different frequencies. Due to short-range interatomic forces, caused by dominances of electrostatic forces in this region, there is anisotropy for which the TO–LO splitting is larger than the A_1–E_1 splitting. The E_2 mode consists of two modes of low and high frequency phonons, assigned as $E_2^{(1)}$(low) and $E_2^{(2)}$(high), which are associated with vibrations of the heavy Zn sublattice and oxygen atoms, respectively. As a result of all of the above, in Table 2 we gather the most typical frequencies and assignation of ZnO Raman active modes [32,33].

Table 2. Frequencies and assignation of typical Raman active modes in ZnO

Frequency for bulk ZnO, cm^{-1}	Assignation of modes
102	$E_2^{(1)}$ (low)
330	Multi phonon
379	A_1(TO)
410	E_1(TO)
437	$E_2^{(2)}$ (high)
541	A_1(LA)
577	A_1(LO)
592	E_1(LO)
660	Multi phonon
1153	Multi phonon

$ZnCo_2O_4$, which has a cubic structure, is a typical representative of normal AB_2O_4 spinel and belongs to the Fd3m (O_h^7) space group with Z = 8. In an ideal AB_2O_4 spinel structure, A atoms are located on tetrahedral sites of T_d symmetry, while B atoms are on octahedral sites of D_{3d} symmetry and oxygen atom occupy C_{3v} sites [34]. In $ZnCo_2O_4$ the anions form a nearly ideal close-packed pseudo-face-center-cubic sublattice surrounded by tetrahedral and octahedral sites where cations occupy only 1/8 of the tetrahedrally coordinated sites and 1/2 of the octahedrally coordinated sites. Theoretical analysis based on factor-group approach predicts, for $ZnCo_2O_4$, five Raman-active bands (A_{1g} + E_g + $3F_{2g}$) and four infrared-active bands F_{1u} [10,35–38]. In Table 3 we gathered frequencies and assignation of Raman active $ZnCo_2O_4$ modes, presented in [35]. Slightly different peak positions for bulk $ZnCo_2O_4$ at 488.0, 525.4, 623.4, 693.0 and ~705 cm^{-1} have been reported in [10] but quantitatively similar to those given in [35], except some of peaks are shifted by up to 10 cm^{-1}.

Table 3. Frequencies and assignation of Raman active modes of $ZnCo_2O_4$ phase

Frequency for $ZnCo_2O_4$ phase, cm^{-1}	Assignation of modes
185	F_{2g}
475	E_g
520	F_{2g}
610	F_{2g}
690	A_{1g}

Figure 1 shows all Raman spectra of samples obtained by hydrothermal method doped with 5 to 50% of CoO. In these spectra, there is an evident existence of modes that belong to both phases, ZnO and $ZnCo_2O_4$. The ZnO phase is represented with its characteristic single phonon modes at 379 (A_1(TO)), 437 ($E_2^{(2)}$), 577 (A_1(LO)), and multi phonons (2LO) at 330, 660 and ~1110 cm^{-1}. The most typical and most obvious representative of ZnO phase, especially in smaller concentrations of CoO, is the mode at 437cm^{-1}. This mode at 437 cm^{-1} behaves the same way as all other ZnO modes; its intensity decreases with increase in CoO concentration. In these spectra, the peak center position is at somewhat lower frequencies than in bulk crystals, due to the nanosized structure of the samples. Beside modes belonging to ZnO, modes such as 185 (F_{2g}), 475 (E_g), 520 (F_{2g}), 610 (F_{2g}) and 690 cm^{-1} (A_{1g}), which represent the $ZnCo_2O_4$ phase, can also be seen. Our results for $ZnCo_2O_4$ modes are in good agreement with results presented in [10] for smaller concentrations of dopant (CoO), while for higher concentration of dopant they are in good agreement with results presented in literature [35]. The intensity of $ZnCo_2O_4$ modes, oppositely from ZnO modes, increased with the increase of CoO concentration. These results of Raman spectroscopy are in good agreement with previously obtained XRD results. Apart from modes that belong to ZnO and $ZnCo_2O_4$, in each and every Raman spectrum of our samples prepared by hydrothermal method, the existence of an additional structure is also evident. This additional structure is the SOP mode, originating from ZnO nanoparticles as a consequence of the nanosize structure of the samples, as mentioned previously.

The effect of change of CoO concentration on the behavior of characteristic SOP modes is shown in Figure 2. It is clearly visible that the intensity of SOP modes decreases with the increase in CoO concentration, which is similar to the intensity behavior of ZnO modes and opposite to intensity behavior of $ZnCo_2O_4$. This conduction of SOP modes is an additional proof that they originate from ZnO.

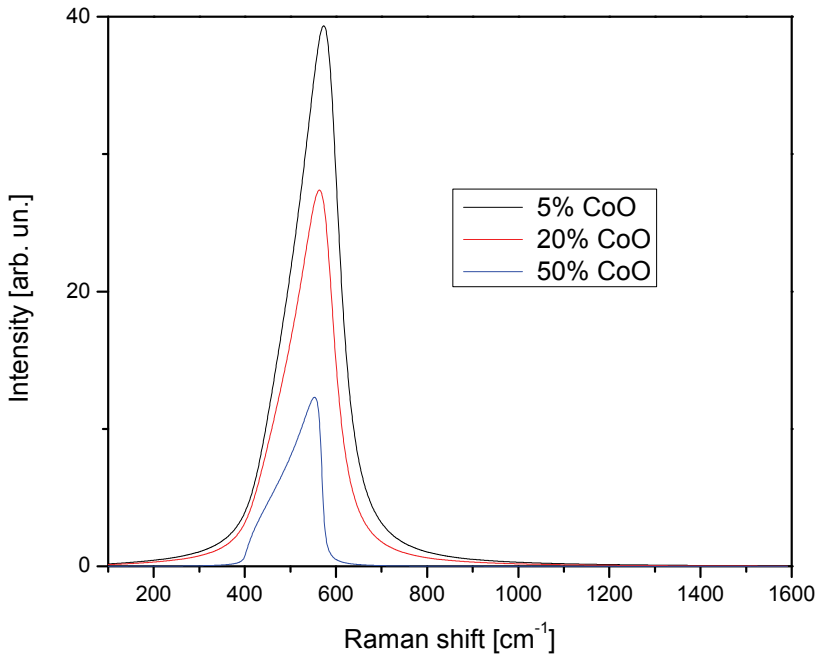

Figure 2. Change of intensity of characteristic SOP modes with CoO concentration.

CONCLUSION

The morphology of hydrothermally obtained samples was examined using SEM, showing particles of different sizes: smaller particles belonging to the $ZnCo_2O_4$ phase, and larger particles belonging to the ZnO phase. The following investigation of phase composition by X-ray diffraction revealed the existence of ZnO and $ZnCo_2O_4$ crystalline phases. In the Raman spectra of all prepared samples, the presence of ZnO was determined by the existence of characteristic single and multi phonons modes. The presence of $ZnCo_2O_4$ was determined by the existence of its typical phonon modes. Besides the modes that belong to $ZnCo_2O_4$ and ZnO phases, there is also evidence of surface optical phonons (SOP) modes. We have investigated the characteristics of the SOP modes and notice that their intensity, as the intensity of ZnO modes, decreased with the increases in CoO concentration, while the intensity of $ZnCo_2O_4$ modes showed the opposite behavior.

REFERENCES

[1] J. Gleize, E. Chikoidze, Y. Dumont, E. Rzepka, O. Gorochov, Superlat. Microstr. **42** (2007) 242–245.

[2] D.F. Wang, S.Y. Park, H.W. Lee, Y.S. Lee, V.D. Lam, Y.P. Lee, Phys. Stat. Sol. (a) **204** (2007) 4029–4032.

[3] Y. Chen, D.M. Bagnall, H. Koh, K. Park, K. Higara, Z. Zhu, T. Yao, J. Appl. Phys. **84** (1998) 3912–3918.

[4] J. Nemeth, G. Rodriguez-Gattorno, A. Diaz, I. Dekany, Langmuir **20** (2004) 2855–2860.

[5] J.M.D. Coey, M. Venkatesan, C.B. Fitzgerald, Nat. Mater. **4** (2005) 173–179.

[6] C. Sudakar, J.S. Thakur, G. Lawes, R. Naik, V.M. Naik, Phys. Rev., B **75** (2007) 054423–054426.

[7] T. Dietl, Acta Phys. Pol., A **111** (2007) 27–46.

[8] R. Cuscó, E. Alarcón-Lladó, J. Ibáñez, L. Artús, J. Jiménez, B. Wang, M.J. Callahan, Phys. Rev., B **75** (2007) 165202––165211.

[9] Y. Liu, J.L. MacManus-Drisoll, Appl. Phys. Lett. **94** (2009) 022503-3.

[10] J. Xu, W.Ji, X.B. Wang, H. Shu, Z.X. Shen, S.H. Tang, J. Raman Spectrosc. **29** (1998) 613–615.

[11] H. Zeng, W. Cai, B. Cao, J. Hu, Y. Li, P. Liu, Appl. Phys. Lett. **88** (2006) 181905-3.

[12] N. Romčević, R. Kostić, B. Hadžić, M. Romčević, I. Kuryliszin-Kudelska, W. Dobrowolski, U. Narkievicz, D. Sibera, JALLCOM **507** (2010) 386–390.

[13] M. Millot, J. Gonzalez, I. Molina, B. Salas, Z. Golacki, J.M. Broto, H. Rakoto, M. Gorian, JALLCOM **423** (2006) 224––227.

[14] R.P. Wang, G. Xu, P. Jin, Phys. Rev., B **69** (2004) 113303-4.

[15] R.Y. Sato-Berrú, A. Vázquez-Olmos, A.L. Fernández-Osorio, S. Sotres-Martínez, J. Raman Spectrosc. **38** (2007) 1073–1076.

[16] P.-M. Chassaing, F. Demangeot, V. Paillard, A. Zwick, N. Combe, C. Pages, M.L. Kahn, A. Maisonnat, B. Chaudret, Phys. Rev., B **77** (2008) 153306-4.

[17] G. Irmer, J. Raman Spectrosc. **38** (2007) 634–646.

[18] A.L. Patterson, Phys. Rev. **56** (1939) 978–982.

[19] A. Ghosh, R.N.P. Choudhary, J. Phys., D **42** (2009) 075416-6.

[20] F. Friedrich, N.H. Nickel, Appl. Phys. Lett. **91** (2007) 111903-3.

[21] C.G. Granqvist, O. Hunderi, Phys. Rev., B **18** (1978) 1554–1561.

[22] K. Karkkainen, A. Saviola, K. Nikoskinen, IEEE Transaction on geosciences and remote sensors **39**(5) (2001) 1013–1018.

[23] J.C.M. Garnett, Trans. R. Soc. Vol. CCIII, 1904, pp. 385––420.

[24] A. Saviola, I. Lindell, Dielectric Properties of Heterogeneous Materials, PIER 6 Progress in Electromagnetic Research, A. Priou, Ed., Elsevier, Amsterdam, 1992.

[25] D.A.G. Bruggeman, Ann. Phys. **24**(5) (1935) 636–679.

[26] J. Saarinen, E.M. Vartiainen, K. Peiponen, Opt. Rev. **10**(2) (2003) 111–115.

[27] X.C. Zeng, D.J. Bergman, P.M. Hui, D. Stroud, Phys. Rev., B **38** (1988) 10970–10973.

[28] J.D. Ye, S. Tripathy, F.F. Ren, X.W. Sun, G.Q. Lo, K.L. Teo, Appl. Phys. Lett. **94** (2009) 011913-3.

[29] I.M. Tiginyanu, A. Sarua, G. Irmer, J. Monecke, S.M. Hubbard, D. Pavlidis, V. Valiaev, Phys. Rev., B **64** (2001) 233317-3.

[30] M. Šćepanović, M. Grujić-Brojčin, K. Vojisavljević, S. Bernik, T. Srećković, J. Raman Spectrosc. **41** (2010) 914––921.

[31] H. Idink, V. Srikanth, W.B. White, E.C. Subbarao, J. Appl. Phys. **76** (1994) 1819–1823.

[32] N. Ashkenov, B.N. Mbenkum, C. Bundesmann, V. Riede, M. Lorenz, D. Spemann, E.M. Kaidashev, A. Kasic, M. Shubert, M. Grundmann, J. Appl. Phys. **93** (2003) 126––133.

[33] E.F. Venger, A.V. Melnichuk, L.L. Melnichuk, Yu.A. Pasechuk, Phys. Stat. Solidi, B **188** (1995) 823–831.

[34] C.M. Julien, M. Massot, J. Phys.: Condens. Matter **15** (2003) 3151–3162.

[35] M. Bouchard, A. Gambardella, J. Raman Spectrosc. **41** (2010) 1477–1485.

[36] X. Wang, R. Zheng, Z. Liu, H. Ho, J. Xu, S.P. Ringer, Nanotechnology **19** (2008) 455702–455708.

[37] O.N. Shebanova, P. Lazor, J. Solid State Chem. **174** (2003) 424–430.

[38] O.N. Shebanova, P. Lazor, J. Chem. Phys. **119** (2003) 6100–6110.

ИЗВОД

РАМАН СПЕКТРОСКОПИЈА ПОВРШИНСКИХ ОПТИЧКИХ ФОНОНА КОД НАНОЧЕСТИЦА ZnO(Co) ДОБИЈЕНИХ ХИДРОТЕРМАЛНОМ МЕТОДОМ

Бранка Хаџић[1], Небојша Ромчевић[1], Maja Ромчевић[1], Izabela Kuryliszyn-Kudelska[2], Witold D. Dobrowolski[2], Ursula Narkiewicz[3], Daniel Sibera[3]

[1]*Институт за физику, Универзитет у Београду, Београд, Србија*
[2]*Institute of Physics, Polish Academy of Science, Warsaw, Poland*
[3]*Institute of Chemical and Environment Engineering, Szczecin University of Technology, Szczecin, Poland*

(Naučni rad)

Узорци ZnO допирани CoO су добијени коришћењем хидротермалне методе. Овакав начин добијања узорака омогућио је настанак серије узорака са различитом концентрацијом допанта од 5 до 50% CoO. Овим узорцима је првобитно испитана морфологија коришћењем скенирајућег електронског микроскопа и при нижим концентрацијама допанта уочене су честице сличних величина, док је са порастом концентрације допанта јасно уочљиво постојање две врсте честица различите величине. Рентгеноструктурном анализом је утврђено порекло ових честица. У нашим узорцима коегзистирају две врсте честица, ZnO и $ZnCo_2O_4$. Такође, ова врста анализе је омогућила да коришћењем Шерерове формуле одредимо средњу величину кристалита ових честица. ZnO честице су величине од 64 до 300 nm, док су $ZnCo_2O_4$ честице величине од 33 до 77 nm. Видимо да величина ZnO честица расте са порастом концентрације допанта док промена величине $ZnCo_2O_4$ честица са концентрацијом није монотона. Вибрационе карактеристике узорака су испитиване коришћењем микро-Раман спектроскопије, зеленом линијом 514,5 nm аргон-јон ласера. Раман спектроскопија је изабрана јер је идеална недеструктивна метода која омогућује испитивање локалног атомског уређења, квалитета узорака, фонона, изотопских ефеката и електрон–фонон спаривања. Добијени Раман спектри су анализирани и фитовани коришћењем Лоренцове линије за све пикове. На овим спектрима, поред карактеристичних пикова за ZnO и $ZnCo_2O_4$ честице, јасно се уочава и додатна структура, за коју смо утврдили да потиче од ZnO, а последица је губитка дугодометне уређености и престанка важења правила симетрије услед нанодимензионалности узорака. Та додатна струкутра су површински оптички фонони (ПОФ). Испитали смо и утицај промене концентрације допанта CoO на понашање ПОФ модова и утврдили да њихов интензитет опада са порастом концентрације CoO, и то за карактеристичне ПОФ модове.

Кључне речи: Нано-материјали • Оптичке особине • Апсорпција и рефлексија светлости • Површински оптички фонони